



# HHS Public Access

Author manuscript

*J Biomed Mater Res B Appl Biomater.* Author manuscript; available in PMC 2020 November 20.

Published in final edited form as:

*J Biomed Mater Res B Appl Biomater.* 2015 January ; 103(1): 39–46. doi:10.1002/jbm.b.33153.

## Effect of fiber orientation of collagen-based electrospun meshes on human fibroblasts for ligament tissue engineering applications

Sean Michael Full<sup>1</sup>, Connor Delman<sup>1</sup>, Jessica M Gluck<sup>1</sup>, Raushan Abdmaulen<sup>2</sup>, Richard J Shemin<sup>1</sup>, Sepideh Heydarkhan-Hagvall<sup>1,3</sup>

<sup>1</sup>Department of Surgery, Division Cardiothoracic Surgery, David Geffen School of Medicine, University of California, Los Angeles, California

<sup>2</sup>Department of Medicine, Division of Cardiology, David Geffen School of Medicine, University of California, Los Angeles, California

<sup>3</sup>AstraZeneca R&D, CVMD iMED Translational Sciences, SE-431 83 Mölndal, Sweden

### Abstract

Within the past two decades polylactic-*co*-glycolic acid (PLGA) has gained considerable attention as a biocompatible and biodegradable polymer that is suitable for tissue engineering and regenerative medicine. In this present study, we have investigated the potential of PLGA, collagen I (ColI), and polyurethane (PU) scaffolds for ligament tissue regeneration. Two different ratios of PLGA (50:50 and 85:15) were used to determine the effects on mechanical tensile properties and cell adhesion. The Young's modulus, tensile stress at yield, and ultimate tensile strain of PLGA(50:50)-ColI-PU scaffolds demonstrated similar tensile properties to that of ligaments found in the knee. Whereas, scaffolds composed of PLGA(85:15)-ColI-PU had lower tensile properties than that of ligaments. Furthermore, we investigated the effect of fiber orientation on mechanical properties and our results indicate that aligned fiber scaffolds demonstrate higher tensile properties than scaffolds with random fiber orientation. Also, human fibroblasts attached and proliferated with no need for additional surface modifications to the presented electrospun scaffolds in both categories. Collectively, our investigation demonstrates the effectiveness of electrospun PLGA scaffolds as a suitable candidate for regenerative medicine, capable of being manipulated and combined with other polymers to create three-dimensional microenvironments with adjustable tensile properties to mimic native tissues.

### Keywords

electrospinning; polylactic-*co*-glycolic acid; polyurethane; collagen I; ligament tissue engineering

## INTRODUCTION

The anterior cruciate ligament (ACL) is the most commonly injured ligament of the knee. More than 250,000 ACL tears occur in the U.S. annually and approximately 150,000 require surgical intervention.<sup>1,2</sup> Ligaments augment joint stability and resist forces to prevent excessive motion. Extracellular matrix (ECM) forms 80% of the tissue volume and fibroblasts make up the remaining 20%. The dry weight of a ligament consists of collagen (75%), elastin (1%), and proteoglycans (20%). Ninety percentage of the collagen is type I and 10% is type III.<sup>3</sup>

It is well established that ligament injuries heal slowly and poorly because of limited vascularization, therefore, requiring surgical intervention.<sup>4</sup> Functional repair or replacement of the ACL remains extremely challenging. Current ACL grafts, such as bone-patellar tendon-bone autograft (BPTB) and hamstring tendon autograft, often lack a combination of flexibility and tensile strength seen in native ACLs.<sup>5</sup> In a survey of 993 physician members of the American Orthopaedic Society for Sports Medicine, 46% commonly preferred BPTB autografts, 32% preferred hamstring autografts, whereas 22% preferred hamstring allografts.<sup>5</sup> Currently, allografts and autografts are the most commonly used methods for reconstruction. The ability for these substitutes to mimic the biomechanical properties of the original ligament is lacking, and although often successful, impaired function and complications are probable.<sup>6,7</sup> Three-dimensional (3D) electrospun polymer scaffolds have come into interest within the past two decades as a means to overcome the limitations associated with current grafts.<sup>7,8</sup> The ideal electrospun scaffold would match the mechanical properties of native ligament tissue, and the material selection would encourage the attachment, proliferation, and migration of ligament fibroblasts.<sup>9</sup> 3D scaffolds offer a fitting alternative due to their ability to overcome the limitations of current surgical procedures. As demonstrated in our present study, various parameters can be manipulated to alter the fiber diameter, porosity, and mechanical tensile strength. This can be utilized to manufacture scaffolds with the necessary characteristics ideal for ligament tissue engineering without the limitations imposed by grafts. The use of biomaterials facilitates the healing process by preventing the need for secondary surgical removal.<sup>10</sup> Three biomaterials that are promising candidates for ligament tissue regeneration are polylactic-*co*-glycolic acid (PLGA), polyurethane (PU), and collagen I (ColI).<sup>11,12</sup>

Collagen scaffolds as well as matrices produced from other natural physiological components are advantageous due to their superior biocompatibility.<sup>13</sup> Collagen is a central component of the ECM of ligaments and tendons, two physiological structures with mechanical properties necessary for the prominent load-bearing forces imposed on musculoskeletal tissues. Difficulty has ensued when attempting to attain biomechanical characteristics similar to that of native tissue.<sup>14</sup> Its natural abundance within ligaments provides an environment similar to the *in vivo* ECM.<sup>15</sup> Collagen also allows for affluent cell proliferation as well as incorporation and retention of extracellular macromolecules. The high retention of extracellular macromolecules in ColI can be attributed to its high porosity. Although advantageous with regards to certain aspects, the highly porous collagen scaffolds may lack the necessary rigidity for withstanding extensive loads.<sup>13</sup> Robayo et al.<sup>16</sup>

demonstrated the viability of ACL fibroblasts in attaching to collagen scaffolds and proliferating successfully through aligned fiber formation.

In addition to collagen, PLGA has also been very well characterized in literature.<sup>17–22</sup> Altering the ratio of polylactic acid (PLA) to polyglycolic acid (PGA) can change the various biomechanical properties and biodegradability of PLGA—the extra methyl group on PLA confers higher hydrophobic and crystalline character, ultimately leading to a slower degradation rate.<sup>23</sup> The crystallinity may be manipulated during the fabrication process by the application of heat, and it has been shown that a 50:50 ratio of PLA to PGA, with low porosity, degrades faster than highly porous samples.<sup>12</sup> The introduction of polycaprolactone (PCL) in a PGA–PCL–PGA triblock decreased crystallinity as well in comparison to isolated PCL scaffolds.<sup>24</sup> Furthermore, its high biocompatibility stems from its nontoxic and natural metabolic byproducts: lactic acid and glycerol.<sup>17</sup> The overall hydrophilicity of PLGA can affect biological responses, such as cell adhesion and proliferation. Fewer cells attach to PLA as a result of its hydrophobic character, but when synthesized with PGA, this drawback can be overcome making PLGA a more suitable candidate. The composition of the hydrophobic and hydrophilic properties of PLGA must be appropriately balanced as to achieve an ideal combination that allows biodegradability as well as biocompatibility and cell proliferation.<sup>25</sup>

3D scaffolds have also been constructed with PU and proved to be of particular interest because of their variable porosity, hydrophilicity, and degradation lifetime.<sup>12</sup> Another beneficial aspect of PU is the ability to easily manipulate the ratio of hydrophobic-to-hydrophilic characteristics, which can be altered during its formation.<sup>12,26</sup> Furthermore, there are other viable methods of increasing cell adhesion and proliferation by use of chemical modifications, such as synthetic peptides.<sup>12</sup> Despite these benefits there are several major limitations with the use of PU. Among these is the inefficiency of macromolecule retention, which could be attributed to large pore size.<sup>27,28</sup> However, lowering pore size on scaffolds could pose another issue of poor nutrient distribution, which leads to poor cell proliferation.<sup>26</sup> Further studies are being carried out on the use of PU but the major limitations seem to suggest that PLGA is the more suitable biomaterial.

Specific to our investigation, we examined the effects of fiber orientation and PLGA ratio on the mechanical properties and cell adhesion of 3D hybrid coaxial scaffolds. Specifically, we measured and compared the Young's modulus, tensile stress at yield, and ultimate tensile strain of PLGA(50:50)-CoII-PU and PLGA(85:15)-CoII-PU scaffolds with aligned and random fiber orientations.

## MATERIALS AND METHODS

### Scaffold fabrication

Electrospinning has been used to produce scaffolds with nano to microdiameter fibers with similar structural properties to the ECM as described in detail before.<sup>29</sup> Briefly, PLGA (85:15 and 50:50) were purchased from Sigma-Aldrich (PLGA, Sigma-Aldrich 430471 and P2191). CoII (CoII, EPC No. C857) was purchased from Elastin Products polyurethane (PU, Fluka 81367) was acquired from Sigma-Aldrich. The selected polymers were used based on

their previously identified abilities to serve as suitable biomaterials for regenerative tissue engineering.<sup>10,11,16</sup> The polymer solutions were prepared by dissolving one another at room temperature in 1,1,1,3,3,3-hexafluoro-2-propanol (HFIP, Sigma-Aldrich 105228–500G) and left overnight until the solution was homogeneous. Two separate samples were electrospun with the following solution properties: (1) 15 w/v % PLGA(85:15), 10 w/v % CoII, and 5 w/v % PU, (2) 15 w/v % PLGA(50:50), 10 w/v % CoII, and 5 w/v % PU. The only variation from the two solutions listed is the substitution of PLGA(85:15 and 50:50)—all other parameters remained constant. With the two solutions, two scaffold types were electrospun: aligned and random oriented fibers.

Two separate 5 mL sterile syringes were loaded, one with the mixed solution of PLGA and CoII and the other with only PU; two needles with diameter of 0.2 and 0.5 mm were used, respectively. The smaller needle tip of the syringe contained the PU solution and was placed inside of the larger needle tip of the syringe, which contained the mixture of PLGA and CoII, forming a needle within a needle set-up that would produce PLGA/CoII fibers with a PU core as shown in (Figure 1). A high voltage supply was used (20 kV; Glassman High Voltage, NJ) with the negative output attached to the needle–needle complex and the positive output attached to rotating mandrel.

First, for the collection of the aligned fiber scaffolds, two parallel copper rods separated by a distance of 8 mm were attached to a rotating mandrel, and fibers were collected at a rotation speed of 500 RPM for 30 min at a solution displacement rate of 50  $\mu$ L/min. The collector was stationed at a fixed distance of ~15 cm away from the needle tip for the duration of the collection.

For the creation of random fiber scaffolds, a stationary copper sheet ( $5 \times 5$  cm<sup>2</sup>) was used as the collection target for the sample solution as opposed to copper rods attached to a rotating drill as used for the creation of aligned fibers. All other parameters were identical to what was listed for the aligned fiber method.

The electrospun scaffolds were cut into ( $1 \times 1$  cm<sup>2</sup>) scaffolds, sanitized in 70% EtOH for 30 min, followed by successive washes with sterile phosphate buffered saline (PBS) for three times prior to cell culturing for 3D *in vitro* studies.

### Scanning electron microscopy

For ultrastructural analysis, unseeded and seeded scaffolds were processed for characterization by scanning electron microscopy (SEM) as described previously.<sup>29</sup> Briefly, cell-seeded samples were rinsed with SEM buffer (0.1 M sodium cacodylate buffer, pH 7.2, supplemented with 5% sucrose) for 10 min. The samples were then fixed for 30 min in 2% paraformaldehyde/2% glutaraldehyde in SEM buffer, followed by dehydration through grades of ethanol, 30, 50, 70, 80, and 95% for 10 min each, followed by three incubations in 100% ethanol for 10 min and a final incubation in 100% ethanol for 40 min. The samples were dried by incubating in one-half volume 100% ethanol and one-half volume hexamethyldisilazane for 20 min followed by 100% hexamethyldisilazane for 20 min. Finally, the 100% hexamethyldisilazane solution was evaporated during 20 min air-drying. Once dry, the samples were mounted onto stubs and sputter coated by gold/palladium

(Au/Pd, thickness of ~10 nm) and SEM images were obtained via JEOL JSM-6490 (JEOL, Peabody, MA) SEM.

### Mechanical testing

The tensile properties of the electrospun 3D fibrous scaffolds were characterized using an Instron mechanical testing instrument (Instron Corporation; Norwood, MA) as described previously.<sup>29</sup> Briefly, the ends of rectangular specimens were mounted vertically between two mechanical gripping units leaving a 6 mm gauge length, and an extension rate of 1 mm/min was then applied. Data from the load-deformation and stress-strain curves were recorded and the tensile stress at maximal load was obtained from these data for each sample. For each fibrous scaffold, at least three rectangular specimens were taken and averaged to determine the tensile properties of the entire scaffold.

### Cell culture and scaffold seeding

Human foreskin fibroblasts (HFF) at passage 4–6 were seeded onto the electrospun scaffolds at a starting density of  $10^6$  cells/cm<sup>2</sup> to reach a confluent cell layer. The HFF-seeded scaffold was then kept in culture for up to 4 weeks under dynamic conditions in DMEM-10% FBS at 37°C and 5% CO<sub>2</sub>.

### Cell count, porosity, and fiber diameter

Cell-seeded scaffolds were also fixed, permeabilized with 0.5% Triton X-100 and nuclei stained with 4'-6-diamidino-2-phenylindole (DAPI). The number of DAPI-stained nuclei on the hybrid coaxial scaffold was counted using ImageJ software (free download available at <http://rsbweb.nih.gov/ij/>). ImageJ was also used to measure the diameter of individual fibers and pores.

### Statistical analysis

Results are presented as mean  $\pm$  standard error of mean. Statistical significance was tested using ANOVA. Probability values of  $p < 0.05$  were considered statistically significant and all data is presented at a  $p < 0.05$  significance level unless otherwise stated.

## RESULTS

### Fiber morphology

**Random fibers.**—Electrospinning using a stationary collector plate produced randomly oriented microfibers for both PLGA(50:50)-CoII-PU and PLGA(85:15)-CoII-PU. Randomly oriented scaffolds of PLGA(50:50)-CoII-PU and PLGA(85:15)-CoII-PU consisted of an average fiber diameter of 2.8  $\mu$ m. The pore size of randomly oriented PLGA(50:50)-CoII-PU fibers consisted of 211.3  $\mu$ m<sup>2</sup>, whereas PLGA(85:15)-CoII-PU fibers measured an average of 174.7  $\mu$ m<sup>2</sup> (Table I and Figure 2).

**Aligned fibers.**—Aligned fiber scaffolds of PLGA(50:50)-CoII-PU and PLGA(85:15)-CoII-PU were produced via a cylindrical rotating collector, described further in the methods section. Morphological analysis of SEM images measured an average fiber diameter of  $0.759 \pm 0.02$  and  $0.712 \pm 0.03$   $\mu$ m, PLGA(50:50)CoII-PU and PLGA(85:15)-CoII-PU. Pore

size measurements were not applicable as aligned fibers produced scaffolds with negligible distance between each individual fiber (Table I, Figure 2).

### Mechanical properties

The effects of aligned and random fibers on mechanical properties were measured and evaluated according to the following categories: Young's modulus (Mpa), tensile stress at yield (Mpa), and tensile strain at maximum (%).

**Tensile strength.**—To accurately compare aligned fibers to ligament tissues, the mechanical properties of aligned fibers were measured both perpendicular ( $\perp$ ) and parallel ( $\parallel$ ) to the length of the fiber. This is consistent with the displacement of tensile stress reflected by anatomical and tibial orientation.<sup>30</sup> Parallel measurements indicate that stress was applied in the direction of the fiber length, whereas perpendicular measurements indicate that stress was applied in the direction of the fiber width. These parameters were not applied toward random fibers due their homogenous nature and thus were not applicable. Measurements are presented in Table II. On average, aligned fibers of either solution type [PLGA(50:50)-ColI-PU and PLGA(85:50)-ColI-PU] demonstrated higher tensile stress and strain than either solution types for random fibers. The highest and lowest mean values corresponding to tensile stress for aligned fibers were  $8.9 \pm 0.68$  MPa [PLGA(50:50)-ColI-PU,  $\perp$ ] and  $1.80 \pm 0.32$  MPa [PLGA(85:15)-ColI-PU,  $\parallel$ ]. This is in contrast to the highest and lowest values for random fibers that corresponded to  $1.16 \pm 0.2$  MPa PLGA(85:15)-ColI-PU and  $0.86 \pm 0.1$  MPa PLGA(50:50)-ColI-PU, suggesting that fiber orientation has an effect on the elastic limit before permanent deformation is exhibited. Furthermore, aligned fiber samples regardless of PLGA ratio demonstrated significantly higher ultimate tensile strain, as shown in Table II.

**Young's modulus.**—Young's modulus was derived based on strain and stress values. It was observed that regardless of fiber orientation, PLGA(85:15)-ColI-PU demonstrated lower values in all corresponding categories in respect to scaffolds composed of PLGA(50:50)-ColI-PU. Young's modulus for random fiber orientation for PLGA(50:50)-ColI-PU and PLGA(85:15)-ColI-PU were  $75.4 \pm 6.3$  MPa and  $20.7 \pm 6.5$  MPa, respectively. Young's modulus for aligned fiber scaffolds were as follows: (50:50,  $\parallel$ ):  $52.1 \pm 13.8$  MPa), (85:15,  $\parallel$ ):  $38.1$  MPa), (50:50,  $\perp$ ):  $348 \pm 12.5$  MPa), and (85:15,  $\perp$ ):  $63.1 \pm 18.2$  MPa). Aligned fiber oriented scaffolds showed a similar trend to random fiber orientation in that fibers composed of PLGA (50:50) showed a higher mean value as opposed to fibers composed of PLGA (85:15), suggesting an increase in Young's modulus when the ratio of polylactic acid is equal to glycolic acid. This also suggests that scaffolds composed of PLGA (50:50) demonstrate higher resistances toward permanent deformation (Table II).

### Cell adhesion

To determine the number of adhered cells to different types of scaffolds, based on the composition and fiber orientation as described earlier, the cell-seeded scaffolds were fixed and nuclei stained with DAPI. The number of DAPI-stained nuclei on the scaffolds was counted using ImageJ software. The data are listed in Figure 3. By day 4, randomly orientated fibers (50:50:  $325.61 \pm 22.81$  cells adhered and 85:15:  $317.25 \pm 34.375$  cells

adhered) showed higher cell adhesion as compared to aligned fiber orientation (50:50:  $285.33 \pm 49.2$  and 85:15:  $271 \pm 37.07$ ). By day 7, scaffolds composed of PLGA(85:15) showed the lowest cell adhesion (Aligned:  $323.25 \pm 26.89$  and Random:  $158 \pm 6.90$ ), whereas the scaffolds composed of PLGA(50:50) began to show an increase in cell adhesion (aligned:  $447 \pm 2.78$  and random:  $427.22 \pm 20.75$ ). By day 14, PLGA(50:50) showed a significant increase in cell adhesion as compared to PLGA(85:15) aligned, PLGA(50:50) random, and PLGA(85:15) random ( $384.5 \pm 4.75$ ,  $343.2 \pm 14.38$ , and  $182.25 \pm 20.27$ , respectively).

## DISCUSSION

Tissue engineering strategy involves the use of biodegradable and biocompatible biomaterials with adequate structural and mechanical properties that can mimic the organization of the native tissue. Other strategies include the use of healthy cells isolated from the patient's own ligaments, or other alternative cell sources such as stem cells and growth factors to regulate the function of these cells. Conceptually, tissue engineering aims to improve the quality of the processes associated with the healing of ligaments by creating viable artificial substitutes in the laboratory that can undergo transplantation to the patient after *in vitro* maturation. Therefore, tissue engineering shows future promise in terms of decreasing the need for ligament grafting procedures while simultaneously reducing the risks associated with them, such as rejection and tissue mismatch, as the construct would carry the patient's own cells.

From the clinical point of view, the main advantages offered by the use of tissue-engineered ligament is minimal patient morbidity, simpler surgical technique, reliable fixation methods, rapid return to preinjury functions, minimal risk for infection or disease transmission, biodegradation at a rate that provides adequate mechanical stability, and support for host tissue ingrowth.<sup>31</sup>

Another important aspect that should be taken into account in the clinical translation of tissue-engineered ligaments is the ligament-bone interface, which consists of a multilayered transition zone. The tissues involved in this interface display distinct mechanical properties; the ligament is strong in tension and bone is strong in compression.<sup>32,33</sup> Therefore, interface is challenging for tissue engineers to mimic, which creates one of the current field of interests in ligament tissue engineering.

The structure and alignment of musculoskeletal tissues leads to their inherent biomechanical properties. It is thusly important to understand the effects on differing the architecture of fiber orientation. This is especially significant as it has been shown that fiber organization governs cell growth and ECM, which in turn can dictate cell differentiation into desired lineages.<sup>34</sup> Aligned fibers, in comparison to randomly oriented fibers, have shown better ligament-like tissue formation.<sup>35</sup> This can be attributed to better cell adhesion because of cell preference to grow lengthwise.<sup>36</sup> The results of our cell attachment test, DAPI staining, showed that electrospun aligned fiber scaffolds containing PLGA had significantly higher cell attachment ( $p < 0.005$ ) than randomly orientated fibers. Teh et al.<sup>37</sup> also demonstrated similar findings that cell adhesion increased in aligned fibers as opposed to random fibers.

This could be attributed to favorable surface morphology for cellular and ECM proliferation.<sup>37,38</sup> Comparison of fluorescent micrographs of DAPI-stained nuclei on PLGA scaffolds demonstrated that aligned fiber scaffolds may provide an optimal microenvironment, which could mimic that of the ECM during cell proliferation. As seen in previous studies, the ECM acts a major influencing factor in cellular support by creating an environment that relays regulatory signals for increased cellular proliferation and attachment.<sup>39</sup> Thus, electrospun scaffolds show great potential in tissue regeneration and engineering by potentially mimicking the critical microenvironment required for cell proliferation, attachment, and differentiation.

Also, pore size has previously been shown to have an effect on cell infiltration as well as nutrient distribution.<sup>40-42</sup> Specifically, Vaquette and Cooper-White<sup>41</sup> demonstrated that an increase in pore size allows a higher cell infiltration and cell adhesion rate. This phenomenon could potentially explain why in our study we observed a decrease in cell adhesion in randomly orientated fibers over a course of 4 weeks while seeing an increase in cell adhesion for aligned fiber scaffolds, which contained negligible-sized pores. Therefore, the decrease in randomly orientated fiber scaffolds could be attributed to cell migration rather than cell detachment or cell death. While aligned fibers mimic the mechanical properties of native ligaments, randomly oriented scaffolds demonstrate better cell infiltration and nutrient distribution. Therefore, fiber orientation can have a significant effect on mechanical properties as well as biocompatibility. In terms of mechanical properties, Yan et al.<sup>43</sup> further demonstrated the effect of fiber alignment in scaffolds by showing that fiber alignment influences mechanical properties in such a way that Young's Modulus is increased. This is attributed to the unidirectional fiber orientation that results in a higher tensile modulus and break strength.

In terms of ligaments, the mechanical properties largely vary by the specific type and age. For example, the human skin has shown an elastic modulus ranging from 15 to 150 MPa, whereas ligaments have been seen at levels of 50 MPa (periodontal),  $250 \pm 28$  MPa (ACL),  $150 \pm 69$  MPa (posterior bundle of PCL), and  $355 \pm 234$  MPa (meniscofemoral).<sup>31,44,45</sup> Jones et al.<sup>27</sup> quantified the biomechanical properties of human ACLs of differing age groups. Failure of middle-aged ligament specimens occurred at loads greater than older-aged specimens (1.6 times the bodyweight compared to 1.3 times the bodyweight).<sup>27</sup> Therefore, age of patient must also be a factor to be considered when determining the most optimal biomaterial for tissue engineering. Noyes and Grood<sup>46</sup> further characterized the force and ultimate strain to failure of human anterior cruciate ligaments. The yield at failure of older individuals (48–86 years) in comparison to younger individuals (16–26 years) was  $4.89 \pm 2.36$  (N·m) and  $12.8 \pm 5.5$  (N·m), respectively. Their corresponding strains were  $48.5 \pm 11.9$  and  $60.25 \pm 6.78$ .<sup>46</sup> This provides a reference for fabricating high quality scaffolds of appropriate biomechanical properties, but is not representative of all musculoskeletal tissues.

In this regard, the mechanical properties exhibited in our study would be sufficient for certain forms of tissue regeneration. Specifically in our scaffold fabrication, PLGA(50:50)-Coll-PU would be suitable in mimicking the mechanical properties of ligament types found in the knee.<sup>31</sup> Our scaffolds composed of PLGA(50:50)-Coll-PU exhibit an elastic modulus ( $348 \pm 12.5$  MPa), ultimate tensile stress ( $8.9 \pm 0.6$  MPa), and strain ( $98.6 \pm 12.28\%$ ) that



would be suitable for tissue engineering. However, of more importance, what our study demonstrates is the potential of PLGA as an effective biocompatible and biodegradable polymer that can be easily manipulated or combined with other polymers to overcome limitations inherent to a specific polymer. This will, in turn, allow the creation of a variety of 3D scaffolds that can cater to and mimic tissue types seen throughout the human body.

Aligned fiber scaffolds do have potential drawbacks including limited and slower cell infiltration resulting from the denser packing and reduced to nonexistent pore size, as seen in our studies as well.<sup>47</sup> Baker et al. showed that aligned PLGA fibers were significantly stiffer than nonaligned fibers.<sup>34,47</sup> However, this could be overcome by varying the ratio of PLGA, as demonstrated by Sahoo et al.,<sup>28</sup> who showed that the increased ratio of Polylactic acid to glycolic acid will produce stiffer scaffolds (higher elastic modulus), which could ultimately lead to lower cell infiltration and adhesion. This may be further extrapolated and generalized to scaffolds synthesized from other polymers or a combination of other polymers.

Thus, to construct optimal scaffolds, the biomechanical properties inherent to native tissue must be determined and it is apparent that native tissues will vary depending on the age of the patient, as shown by the varying degree of elastic modulus in ligaments compared to age.  
30

## CONCLUSIONS

In our present study, we have shown that aligned fiber scaffolds demonstrated significantly higher tensile properties than that of randomly orientated fibers. Still, the ideal replacement scaffold for any tissue type must be sufficiently porous to facilitate cell perfusion and nutrient distribution of seeded cells. Therefore, pore size, fiber diameter, fiber orientation, and polymer combination are all factors for consideration that affect the cell viability and mechanical properties of a scaffold.

Electrospun aligned fiber scaffolds composed of PLGA(50:50)-Coll-PU have exhibited higher tensile properties than that of scaffolds composed of PLGA(85:15)-Coll-PU. In this regard, PLGA(50:50)-Coll-PU demonstrates the potential for use in tissue engineering requiring tensile properties similar to ligaments found in the knee: ACL, posterior cruciate ligament (PCL), and medial cruciate ligament (MCL), whereas PLGA(85:15)-Coll-PU demonstrates mechanical suitability for tissue demonstrating a lower elastic modulus.

Although we focus on comparing specific polymer combinations and their effects on mechanical properties suitable for tissue regeneration, the larger goal of our present study is to demonstrate the potentials of PLGA as an effective polymer that can be easily manipulated and combined with other polymers to fabricate 3D scaffolds suitable for a variety of tissue types seen throughout the human body.

## ACKNOWLEDGMENTS

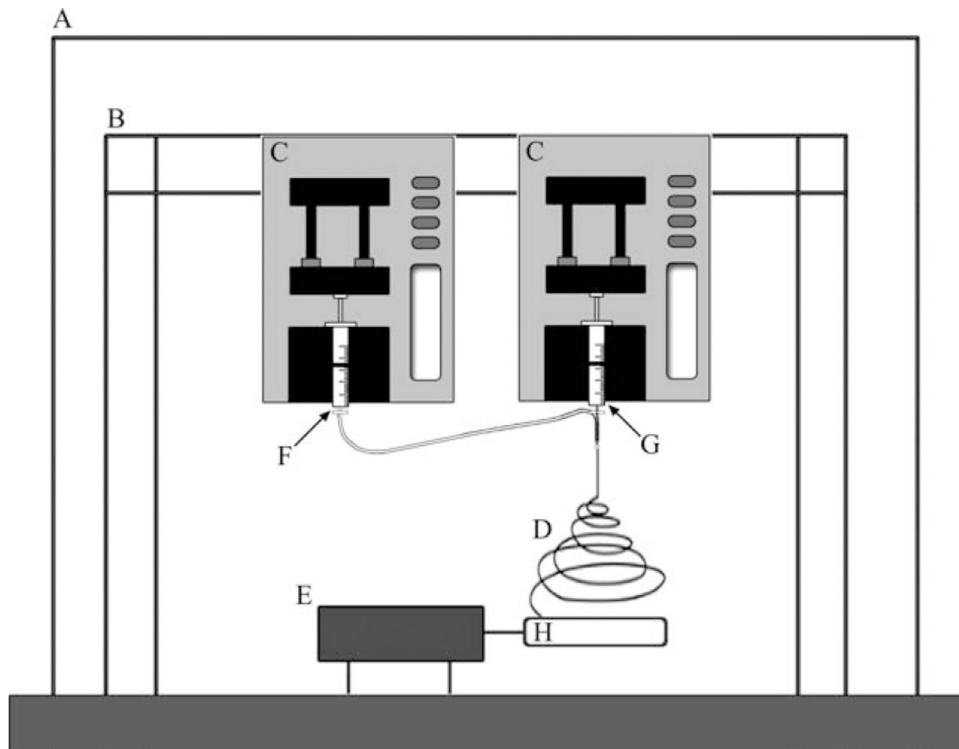
This work was supported by the Department of Surgery at UCLA.

## REFERENCES

1. Cooper JA, Lu HH, Ko FK, Freeman JW, Laurencin CT. Fiber-based tissue-engineered scaffold for ligament replacement: Design considerations and in vitro evaluation. *Biomaterials* 2005;26:1523–1532. [PubMed: 15522754]
2. Cooper JA, Bailey LA, Carter JN, Castiglioni CE, Kofron MD, Ko FK, Laurencin CT. Evaluation of the anterior cruciate ligament, medial collateral ligament, Achilles tendon and patellar tendon as cell sources for tissue-engineered ligament. *Biomaterials* 2006;27: 2747–2754. [PubMed: 16414115]
3. Carlstedt C, Nordin M. Biomechanics of tendons and ligaments In: Nordin M and Frankel VH, editors. *Basic Biomechanics of the Musculoskeletal System*. Malvern, PA: Lea & Febiger; 1989 pp 59–74.
4. Laurencin C, Freeman J. Ligament tissue engineering: An evolutionary materials science approach. *Biomaterials* 2005;2:7530–7536.
5. Duquin TR, Wind WM, Fineberg MS, Smolinski RJ, Buyea CM. Current trends in anterior cruciate ligament reconstruction. *J Knee Surg* 2009;22:7–12. [PubMed: 19216345]
6. Cooper JA, Sahota JS Jr, Gorum WJ, Carter J, Doty SB, Laurencin CT. Biomimetic tissue-engineered anterior cruciate ligament replacement. *Proc Natl Acad Sci USA* 2007;104:3049–3054. [PubMed: 17360607]
7. Lu HH, Cooper JA, Manuel S, Freeman JW, Attawia MA, Ko FK, Laurencin CT. Anterior cruciate ligament regeneration using braided biodegradable scaffolds: In vitro optimization studies. *Biomaterials* 2005;26:4805–4816. [PubMed: 15763260]
8. Makadia HK, Siegel SJ. Poly Lactic-co-glycolic acid (PLGA) as biodegradable controlled drug delivery carrier. *Polymers* 2011;3: 1377–1397. [PubMed: 22577513]
9. Liu Y, Ramanath HS, Wang DA. Tendon tissue engineering using scaffold enhancing strategies. *Trends Biotechnol* 2008;26:201–209. [PubMed: 18295915]
10. Athanasiou KA, Agrawal CM, Barber FA, Burkhart SS. Orthopaedic applications for PLA-PGA biodegradable polymers. *Arthroscopy* 1998;14:726–737. [PubMed: 9788368]
11. Gentleman E, Lay AN, Dickerson DA, Nauman EA, Livesay GA, Dee KC. Mechanical characterization of collagen fibers and scaffolds for tissue engineering. *Biomaterials* 2003;24:3805–3813. [PubMed: 12818553]
12. Grad S, Kupcsik L, Gorna K, Gogolewski S, Alini M. The use of biodegradable polyurethane scaffolds for cartilage tissue engineering: Potential and limitations. *Biomaterials* 2003;24:5163–5171. [PubMed: 14568433]
13. Glowacki J, Mizuno S. Collagen scaffolds for tissue engineering. *Biopolymers* 2008;89:338–44. [PubMed: 17941007]
14. Kew SJ, Gwynne JH, Enea D, Abu-Rub M, Pandit A, Zeugolis D, Brooks RA. Regeneration and repair of tendon and ligament tissue using collagen fibre biomaterials. *Acta Biomater* 2011;7:3237–3247. [PubMed: 21689792]
15. Goulet F, Chabaud S, Simon F, Napa ID, Moulin V, Hart DA. Potential of tissue-engineered ligament substitutes for ruptured ACL replacement. *Intech* 2011;9:163–178.
16. Robayo LM, Moulin VJ, Tremblay P, Cloutier R, Lamontagne J, Larkin AM, Chabaud S, Simon F, Islam N, Goulet F. New ligament healing model based on tissue-engineered collagen scaffolds. *Wound Repair Regen* 2011;19:38–48. [PubMed: 21143691]
17. Astete CE, Sabliov CM. Synthesis and characterization of PLGA nanoparticles. *J Biomater Sci Polym Ed* 2006;17:247–289. [PubMed: 16689015]
18. Pan Z, Ding J. Poly(lactide-co-glycolide)porous scaffolds for tissue engineering and regenerative medicine. *Interface Focus* 2012;2: 366–377. [PubMed: 23741612]
19. Baek MO, Kim SH, So JW, Lim JY, Choi JH, Rhee JM, Lee HB, Khang G. Fabrication and characterization of PLGA scaffold penetrated with demineralized bone solution. *Tissue Eng Regen Med* 2008;5:229–234.
20. Sahoo SK, Panda AK, Labhasetwar V. Characterization of porous PLGA/PLA microparticles as scaffold for three dimensional growth of breast cancer cells. *Biomacromolecules* 2005;6:1132–1139. [PubMed: 15762686]

21. Nie H, Wang CH. Fabrication and characterization of PLGA/Hap composite scaffolds for delivery of BMP-2 plasmid DNA. *J Control Release* 2007;120:111–121. [PubMed: 17512077]
22. Razak S, Sharif N, Rahman W. Biodegradable polymers and their bone applications: A review. *Int J Basic Appl Sci* 2012;12: 31–49.
23. Mikos AG, Temenoff JS. Formation of highly porous biodegradable scaffolds for tissue engineering. *Electron J Biotechnol* 2000; 3:1995–2000.
24. Chung AS, Hwang HS, Das D, Zuk P, McAllister DR, Wu BM. Lamellar stack formation and degradative behaviors of hydrolytically degraded poly( $\epsilon$ -caprolactone) and poly(glycolide- $\epsilon$ -caprolactone) blended fibers. *J Biomed Mater Res* 2012;100: 274–284.
25. Ouyang HW, Goh JCH, Mo XM, Teoh SH, Lee EH. Characterization of anterior cruciate ligament cells and bone marrow stromal cells on various biodegradable polymeric films. *Mater Sci Eng* 2002;20:63–69.
26. Allemann F, Mizuno S, Eid K, Yates KE, Zaleske D, Glowacki J. Effects of hyaluronan on engineered articular cartilage extracellular matrix gene expression in 3-dimensional collagen scaffolds. *J Biomed Mater Res* 2001;55:13–19. [PubMed: 11426390]
27. Jones RS, Nawana NS, Pearcy MJ, Learmonth DJA, Bickerstaff DR, Costi JJ, Paterson RS. Mechanical properties of the human anterior cruciate ligament. *Clin Biomech* 1995;10:339–344.
28. Sahoo S, Ouyang HW, Goh JC, Tay TE, Toh SL. Characterization of a novel polymeric scaffold for potential application in tendon/ligament tissue engineering. *Biomaterials* 2008;29:662–674.
29. Gluck JM, Rahgozar P, Ingle NP, Rofail F, Petrosian A, Cline MG, Jordan MC, Roos KP, Maclellan WR, Shemin RJ, Heydarkhan-Hagvall S. Hybrid coaxial electrospun nanofibrous scaffolds with limited immunological response created for tissue engineering. *J Biomed Mater Res B Appl Biomater* 2011;99:180–90. [PubMed: 21732530]
30. Woo SL, Hollis M, Adams DJ, Lyons RM, Takai S. Tensile properties of the human femur-anterior cruciate ligament-tibia complex. The effects of specimen age and orientation. *Am J Sports* 1991;9:217–25.
31. Vunjak-Novakovic G, Altman G, Horan R, Kaplan DL. Tissue engineering of ligaments. *Annu Rev Biomed Eng* 2004;6:131–156. [PubMed: 15255765]
32. Martin RB, Burr DB, Sharkey NA. *Skeletal Tissue Mechanics*, New York, NY: Springer; 1998.
33. Wang JHC. Mechanobiology of tendon. *J Biomech* 2006;39:1563–1582. [PubMed: 16000201]
34. Baker BM, Mauck RL. The effect of nanofiber alignment on the maturation of engineered meniscus constructs. *Biomaterials* 2007; 28:1967–1977. [PubMed: 17250888]
35. Bashu CA, Shaffer RD, Dahlgren LA, Guelcher SA, Goldstein AS. Effect of fiber diameter and alignment of electrospun polyurethane meshes on mesenchymal progenitor cells. *Tissue Eng* 2009;15:2435–2445.
36. Teh R, Toh S, Goh J. Aligned hybrid silk scaffold for enhanced differentiation of mesenchymal stem cells into ligament fibroblasts. *Tissue Eng* 2011;17:687–703.
37. Teh T, Toh S-L, Goh J. Aligned hybrid silk scaffold for enhanced differentiation of mesenchymal stem cells into ligament fibroblasts. *Tissue Eng: Part C* 2011;17:687–703.
38. Lee CH, Shin HJ, Cho IH, Kang I-M, Kim IA, Park D-K, Shin J-W. Nanofiber alignment and direction of mechanical strain affect the ECM production of human ACL fibroblast. *Biomaterials* 2005;26: 1261–1270. [PubMed: 15475056]
39. Sherr EB, Caron DA, Sherr BF. Staining of heterotrophic protists for visualization via epifluorescence microscopy In: Kemp P, Sherr B, Sherr E, Cole J, editors. *Handbook of Methods in Aquatic Microbial Ecology*. NY: Lewis Publ.; 1993 pp. 213–228.
40. Huang M, Wang Y, Luo Y. Biodegradable and bioactive porous polyurethanes scaffolds for bone tissue engineering. *J Biomed Sci Eng* 2009;2:36–40.
41. Vaquette C, Cooper-White JJ. Increasing electrospun scaffold pore size with tailored collectors for improved cell penetration. *Acta Biomater* 2011;7:2544–2557. [PubMed: 21371575]
42. Murphy C, O'Brien F. Understanding the effect of mean pore size on cell activity in collagen-glycosaminoglycan scaffolds. *Cell Adhes Migr* 2010;4:377–381.

43. Yan J, Qiang L, Gao Y, Cui X, Zhou H, Zhong S, Wang Q, Wang H. Effect of fiber alignment in electrospun scaffolds on keratocytes and corneal epithelial cells behavior. *J Biomed Mater Res Part A* 2012;100A:527–535.
44. Li WJ, Laurencin CT, Catterson EJ, Tuan RS, Ko FK. *J Biomed Mater Res* 2002;60:613–621. [PubMed: 11948520]
45. Rees JS, Jacobsen PH. Elastic modulus of the periodontal ligament. *Biomaterials* 1997;18:995–999. [PubMed: 9212195]
46. Noyes FR, Grood ES. The strength of the anterior cruciate ligament in humans and rhesus monkeys. *Surgery* 1976;58:1074–1082.
47. Baker BM, Gee AO, Metter RB, Nathan AS, Marklein L, Burdick JA, Mauck RL. The potential to improve cell infiltration in composite fiber-aligned electrospun scaffolds by the selective removal of sacrificial fibers. *Biomaterials* 2009;29:2348–2358.

**FIGURE 1.**

Schematic set-up of two-syringe system for electrospinning bicomponent fiber scaffolds. A: chemical fume hood. B: Support beams used to holster electrospinning syringe pumps. C: Syringe pumps. D: Electrospun fibers. E: Rotating drill system for aligned fiber production. F: 5 w/v % PU. G: 15 w/v % PLGA and 10 w/v % CoII. H: Static collector.

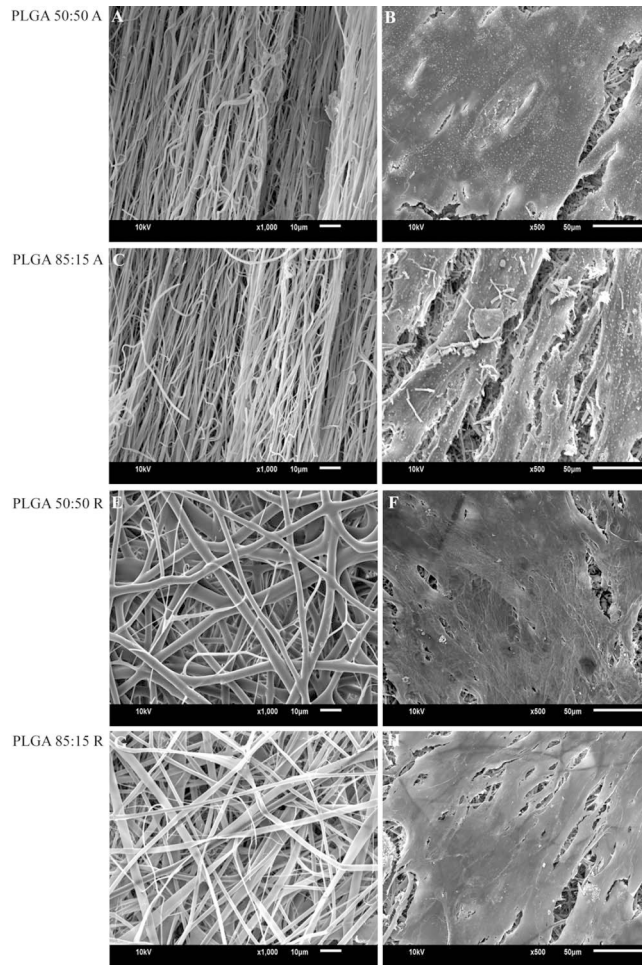


**FIGURE 2.** (A and C): Scanning electron micrograph of aligned fiber scaffolds. (B and D): Cell-seeded scaffolds (2 weeks in culture). (E and G): Scanning electron micrograph of random fiber scaffolds. (F and H): Cell-seeded scaffolds (2 weeks in culture).

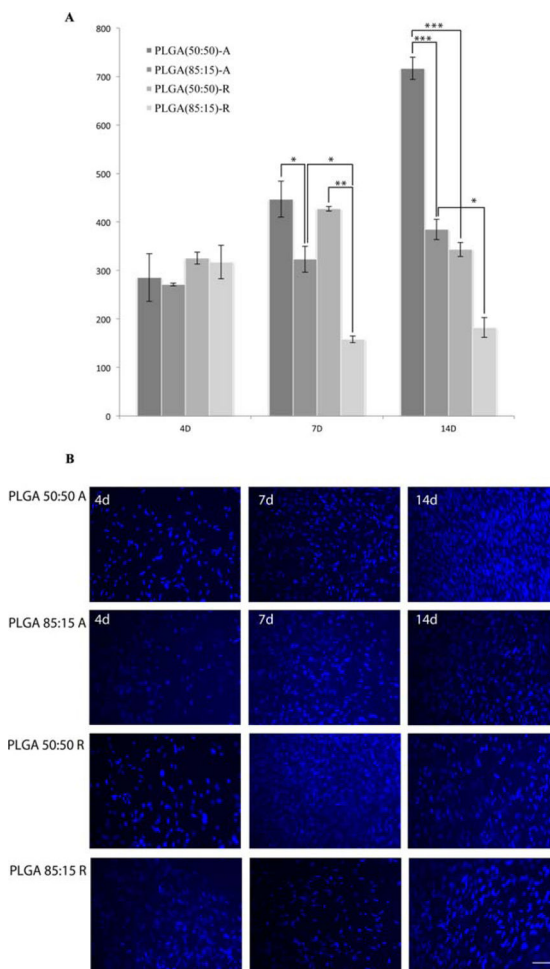


**FIGURE 3.**

A: Cell adhesion assay measured at days 4, 7, and 14. Bars represented as mean  $\pm$  standard error of mean. Figure legend indicates scaffold composition as well as fiber orientation: A—Aligned and R—Random. Asterisks represent statistical significance: \* $p < 0.05$ , \*\* $p < 0.005$ , and \*\*\* $p < 0.0005$ . B: HFF seeded on scaffolds for 4, 7, and 14 days and nuclei stained using DAPI (blue), scale bar 20  $\mu\text{m}$ . [Color figure can be viewed in the online issue, which is available at [wileyonlinelibrary.com](http://wileyonlinelibrary.com).]

**TABLE I.**

Average Fiber Diameter and Pore Size of Hybrid Co-Axial Scaffolds of PLGA-CoII-PU

<b>Fiber Types</b>	<b>Fiber Diameter (<math>\mu\text{M}</math>)</b>	<b>Pore Size (<math>\mu\text{M}^2</math>)</b>
Aligned Fibers		
PLGA (50:50)	$0.759 \pm 0.025$	$4.67 \pm 0.46$
PLGA (85:15)	$0.712 \pm 0.031$	$6.75 \pm 0.75$
Random Fibers		
PLGA (50:50)	$2.82 \pm 0.68$	$211.3 \pm 31.1$
PLGA (85:15)	$1.92 \pm 0.58$	$174.7 \pm 34.9$

All measurements represent the mean  $\pm$  standard error of mean of 50 fiber diameter and pore size measurements.

Author Manuscript

Author Manuscript

Author Manuscript

Author Manuscript



**TABLE II.**

Mechanical Properties of Aligned and Random Hybrid Co-Axial PLGA-Coll-PU Scaffolds

Sample Type	Young's Modulus (MPa)	Ultimate Tensile Strain (%)	Tensile Stress at Yield (MPa)
Aligned Fiber PLGA (50:50)			
Perpendicular	348.38 ± 12.5	98.61 ± 12.28	8.98 ± 0.68
Parallel	52.46 ± 13.8	79.48 ± 1.88	2.46 ± 0.64
Aligned Fiber PLGA (85:15)			
Perpendicular	63.12 ± 18.22	91.36 ± 17.31	7.09 ± 1.9
Parallel	38.11 ± 6.8	82.99 ± 23.41	1.80 ± 0.32
Random Fiber PLGA (50:50)			
	75.4 ± 6.3	28.55 ± 1.47	0.86 ± 0.11
Random Fiber PLGA (85:15)			
	20.76 ± 6.5	56.16 ± 2.31	1.17 ± 0.21

All results are shown as mean ± standard error of the mean ( $n = 25$ ).